Environmental Science and Pollution Research (2024) 31:50347–50358
https://doi.org/10.1007/s11356-024-34374-8

RESEARCH ARTICLE

Atmospheric chemistry of $CF_3CHFCF_2OCH_3$ (HFE-356mec3) and $CHF_2CHFOCF_3$ (HFE-236ea1) initiated by OH and Cl and their contribution to global warming

Sara Espinosa[1,2] · María Asensio[1,2] · María Antiñolo[1,2] · José Albaladejo[1,2] · Elena Jiménez[1,2]

Received: 25 January 2024 / Accepted: 9 July 2024 / Published online: 2 August 2024

Abstract

The kinetic study of the gas-phase reactions of hydroxyl (OH) radicals and chlorine (Cl) atoms with $CF_3CHFCF_2OCH_3$ (HFE-356mec3) and $CHF_2CHFOCF_3$ (HFE-236ea1) was performed by the pulsed laser photolysis/laser-induced fluorescence technique and a relative method by using Fourier Transform infrared (FTIR) spectroscopy as detection technique. The temperature dependences of the OH-rate coefficients ($k_{OH}(T)$ in cm^3s^{-1}) between 263 and 353 K are well described by the following expressions: $9.93\times10^{-13}\exp\{-(988\pm35)/T\}$ for HFE-356mec3 and $4.75\times10^{-13}\exp\{-(1285\pm22)/T\}$ for HFE-236ea1. Under NO_x-free conditions, the rate coefficients k_{Cl} at 298 K and 1013 mbar (760 Torr) of air were determined to be $(2.30\pm1.08)\times10^{-13}$ cm^3s^{-1} and $(1.19\pm0.10)\times10^{-15}$ cm^3s^{-1}, for HFE-356mec3 and HFE-236ea1, respectively. Additionally, the relative kinetic study of the $Cl+CH_2ClCHCl_2$ reaction was investigated at 298 K, as it was used as a reference reaction in the kinetic study of the Cl-reaction with HFE-356mec3 and discrepant rate coefficients were found in the literature. The global atmospheric lifetimes were estimated relative to CH_3CCl_3 at the tropospheric mean temperature (272 K) as 1.4 and 8.6 years for HFE-356mec3 and HFE-236ea1, respectively. These values combined with the radiative efficiencies for HFE-356mec3 and HFE-236ea1 derived from the measured IR absorption cross sections (0.27 and 0.41 W m^{-2} ppv^{-1}) yield global warming potentials at a 100-yrs time horizon of 143 and 1473, respectively. The contribution of HFE-356mec3 and HFE-236ea1 to global warming of the atmosphere would be large if they become widespread increasing their atmospheric concentration.

Keywords GHG replacements · Atmospheric reactivity · Atmospheric lifetimes · Radiative efficiency · Global warming potential · Climate change

Introduction

Hydrofluoroethers (HFEs) have been presented in the last decades as potential substitutes of chlorofluorocarbons (CFCs) and hydrochlorofluorocarbons (HCFCs) in many industrial applications (Tsai 2005). To evaluate the environmental impact produced by their potential widespread emissions, it is necessary to know a priori the atmospheric lifetime due to gas-phase homogeneous reactions with oxidants (*e.g.,* OH radicals, Cl atoms, ozone, etc.) and UV photolysis in the actinic region. In addition, it is important to know its contribution to the global warming of the atmosphere, since HFEs strongly absorb the infrared (IR) radiation within the so-called "IR atmospheric window" (700–1250 cm^{-1}).

In this work, we present the gas-phase kinetics of the reactions of 1,1,2,3,3,3-hexafluoropropyl methyl ether ($CF_3CHFCF_2OCH_3$, HFE-356mec3) and 1,2,2-trifluoroethyl trifluoromethyl ether ($CHF_2CHFOCF_3$, HFE-236ea1) with

Responsible Editor: Gerhard Lammel

Highlights
- HFE-356mec3 and HFE-236ea1 react slowly with OH and Cl at 298 K.
- Activation energies for OH-reactions were 8.2 and 10.7 kJ mol^{-1} for HFE-356mec3 and HFE-236ea1.
- They absorb in the mid-IR (500-1500 cm^{-1}) with peak absorption cross-sections ~ 10^{-18} cm^2 $molecule^{-1}$.
- Lifetime-corrected radiative efficiencies of the investigated HFEs were 0.27 and 0.41 W m^{-2} $ppbv^{-1}$.
- Even the investigated HFEs still present relatively high $GWP_{100\text{-yrs}}$, it is reduced with respect to analogue HFCs.

Extended author information available on the last page of the article

OH radicals as a function of temperature (263–353 K) and at 66.66 and 133.32 mbar (i.e., 50 and 100 Torr) of helium using the pulsed laser photolysis-laser induced fluorescence (PLP-LIF) technique.

$$OH + CF_3CHFCF_2OCH_3 \rightarrow \text{Products} \quad \text{(R1)}$$

$$OH + CHF_2CHFOCF_3 \rightarrow \text{Products} \quad \text{(R2)}$$

with respect to the kinetics of reaction (R1), Urata et al. (2003) reported an estimate for the rate coefficient at room temperature, k_{OH}(298 K), but no measurement has been reported yet. Therefore, an experimental study is needed to confirm the estimation of Urata et al. (2003). On the other hand, for reaction (R2), there is only a relative measurement of k_{OH}(298 K) reported by Oyaro et al. (2005) at 1013 mbar of air using gas chromatography-mass spectrometry (GC–MS) as detection technique.

There are also limited literature data on the kinetic study of the Cl-reaction of HFE-356mec3 (R3) and HFE-236ea1 (R4).

$$Cl + CF_3CHFCF_2OCH_3 \rightarrow \text{Products} \quad \text{(R3)}$$

$$Cl + CHF_2CHFOCF_3 \rightarrow \text{Products} \quad \text{(R4)}$$

As far as we know, there is only an absolute kinetic study on reaction (R3) as a function of temperature (263–363 K) using a very low-pressure reactor (< 4 mbar) and a quadrupole mass spectrometry for monitoring HFE-356mec3 (Papadimitriou et al. 2004). No data at tropospheric pressures are available to date. Regarding reaction (R4), Oyaro et al. (2005) employed a relative kinetic method using GC–MS to monitor HFE-236ea1 and the reference compound to measure k_{Cl} at room temperature, k_{Cl}(298 K), and 1013 mbar of air. These authors reported an average value of k_{Cl}(298 K) of $(1.2 \pm 2.0) \times 10^{-15}$ cm^{3}s^{-1}, with extremely large uncertainties (ca. 200%). Hence, an additional measurement of k_{Cl}(298 K) is desired to clarify this point and to reduce the uncertainty.

The present study presents (*i*) the first absolute measurement of $k_{OH}(T)$ for reactions (R1) and (R2) as a function of T (263–353 K) and between 66.66 and 133.32 mbar using PLP-LIF, from which the Arrhenius parameters were derived; (*ii*) a revision of the relative kinetics of reactions (R3) and (R4) using different reference compounds; and (*iii*) an estimation of the atmospheric lifetime of HFE-356mec3 and HFE-236ea1 from k_{OH}(272 K) and k_{Cl}(298 K) for global atmosphere, and from k_{OH}(298 K) and k_{Cl}(298 K) for a coastal atmosphere at dawn.

Although HFEs are not expected to absorb radiation at $\lambda > 200$ nm (Orkin et al. 1999), the UV spectra of HFE-236ea1 and HFE-356mec3 were measured in this work between 190 and 400 nm. The absorption cross section (σ_λ) at 248 nm was determined for HFE-356mec3 and HFE-236ea1 to assess their potential photolysis during the absolute kinetic experiments. Regarding the IR absorption cross sections ($\sigma_{\tilde{\nu}}$) in the mid-infrared region, Le Bris et al. (2020) determined this parameter for HFE-356mec3 between 550 and 3500 cm^{-1}. Oyaro et al. (2005) reported $\sigma_{\tilde{\nu}}$ for HFE-236ea1 in a similar wavenumber range (400–3200 cm^{-1}). These authors also provided global warming potential (*GWP*) calculations (Le Bris et al. 2020; Oyaro et al. 2005). In the present work, Fourier transform infrared (FTIR) spectroscopy was used to reinvestigate the IR spectra of the titled HFEs between 500 and 4000 cm^{-1}. Based on the results obtained in this work, the lifetime-corrected radiative efficiencies (*REs*) and *GWPs* relative to CO_2 for both HFEs were reexamined.

Experimental set-ups and techniques

Absolute gas-phase kinetics of OH-reactions

The experimental system and procedure to determine the second-order rate coefficient $k_{OH}(T)$ has been explained elsewhere (Albaladejo et al. 2002; Antiñolo et al. 2012; Blázquez et al. 2017). Briefly, the pulsed laser photolysis at 248 nm of hydrogen peroxide (H_2O_2) was employed to generate in situ OH radicals in a 200 cm^3 jacketed Pyrex® cell. The monitoring of the electronic ground state OH was performed by laser induced fluorescence at 310 nm, emitted from excited OH radicals at 282 nm. Under *pseudo*-first order conditions (*i.e.* HFE in large excess with respect to OH), the LIF signal (I_{LIF}) follows a single exponential function. Some examples of the temporal evolution of I_{LIF} are shown in Figure S1 of the supporting information (SI). From the analysis of such decays, the *pseudo*-first order coefficient (k') for a given HFE concentration, temperature, and pressure (p_T) is obtained. The loss of OH in the absence of HFE is due to reaction with H_2O_2 or diffusion out of the detection zone (k'_0), as shown in Eq. E1.

$$k' - k'_0 = k_{OH}(T)[\text{HFE}] \quad \text{(E1)}$$

The second-order rate coefficient $k_{OH}(T)$ for reactions (R1) and (R2) is obtained from k'-k'_0 versus [HFE] plots. p_T was set to 133.32 mbar of helium except for the experiments carried out at 298 K, where experiments were also performed at 66.66 mbar. All gases were introduced into the reactor by calibrated mass flow controllers (MFCs), particularly important for the HFE/He mixtures. An example of the calibration of the mass rate flow (F_R) of the relatively concentrated HFE mixtures (9.8–10.4% for HFE-356mec3 and 25.5% for HFE-236ea1) from the storage bulb is shown in Figure S2. As shown, the "real" mass flow rate is much lower than the set one (50% for HFE-356mec3 and 66% for HFE-236ea1). By changing F_R and the total flow rate, [HFE] in the reactor was varied ([HFE-356mec3] = $(0.36–8.12) \times 10^{16}$ cm^{-3} and [HFE-236ea1] = $(0.06–2.08) \times 10^{17}$ cm^{-3}).

Relative kinetics for Cl-reactions

The experimental system and procedure to determine k_{Cl}(298 K) has been described elsewhere (Antiñolo et al. 2020; Asensio et al. 2022, 2023; Ballesteros et al. 2017; Ceacero-Vega et al. 2012). Briefly, it consists of a White-type Pyrex gas cell (V = 16 L) with an optical pathlength of (59.0 ± 4.9) m, which is surrounded by 3 actinic lamps (Philips Actinic BL TL 40W/10 1SL/25, λ = 340–400 nm) to generate Cl atoms in situ by photolysis of Cl_2. The cell is coupled to a FTIR spectrometer (Thermo Nicolet, Nexus 870) with a liquid N_2-cooled MCT (Mercury Cadmium Telluride) detector. In the kinetic study of reaction (R3), methane (CH_4) and 1,2,2-trichloroethane ($CH_2ClCHCl_2$) were used as reference compounds, while for reaction (R4) due to the difficulty of finding a suitable reference compound, only 1,1,1-trichloroethane (CH_3CCl_3) was used. As discrepant k_{Cl}(298 K) values for $CH_2ClCHCl_2$ (reaction (R5)) were found in the literature, we decided to determine it before using $CH_2ClCHCl_2$ as a reference compound to study reaction (R3).

$$Cl + CH_2ClCHCl_2 \rightarrow \text{Products} \quad \text{(R5)}$$

The reference compounds used in these preliminary kinetic experiments were CH_4 and dichloromethane (CH_2Cl_2).

Considering all loss processes for the HFE and the reference compound, the integrated rate equation is given by:

$$ln\left(\frac{[HFE]_0}{[HFE]_t}\right) - k_{loss}t = \frac{k_{Cl}(298K)}{k_{ref}}\left[\ln\left(\frac{[Ref]_0}{[Ref]_t}\right) - k_{Ref,loss}t\right] \quad \text{(E2)}$$

k_{ref} refers to the rate coefficient for the Cl-reaction with the reference compound at 298 K and 1013 mbar; $[HFE]_0$, $[HFE]_t$, $[Ref]_0$ and $[Ref]_t$ are the concentrations of the HFE and the reference compound at the beginning of the reaction and at a reaction time t, respectively. k_{loss} and $k_{Ref,loss}$ are the first-order rate coefficients for the secondary losses for the HFE and the reference compound, respectively. [HFE] and [Ref] were measured by FTIR spectroscopy. $[HFE]_0$ and $[Ref]_0$ are listed in Table S3. The IR spectra were recorded in the 650–4000 cm^{-1} range under static conditions and at an instrumental resolution of 2 cm^{-1}. They were recorded every 2 min during 130 min for HFE-356mec3, 150 min for HFE-236ea1 and 90 min for $CH_2ClCHCl_2$. k_{loss} and $k_{Ref,loss}$ (Table S4) were measured prior to each experiment and include heterogeneous losses, photolysis and/or reaction with Cl_2, as described in previous works (Antiñolo et al. 2020; Asensio et al. 2022).

UV and IR absorption spectroscopy in the gas-phase

The UV absorption spectroscopy system has been described in detail elsewhere (Asensio et al. 2022; Blázquez et al. 2020). It consists of a deuterium lamp (StellarNet, SL4 DT-200) placed at the entrance of a jacketed Pyrex® cell (optical path length, ℓ = (107.0 ± 0.5)cm), connected by an optical fiber to a *f*/2 spectrograph (StellarNet, BLK-C) that possesses a concave holographic grating (590 grooves/mm) and a slit of 100 µm The transmitted intensity was detected in a charge-coupled device detector (2048 pixels). The UV cell was filled with pure HFE-356mec3 (38–71 mbar ≡ 28.67–53.35 Torr), and HFE-236ea1 (92–133 mbar ≡ 68.68–99.76 Torr), resulting in [HFE] ranges of (0.93–1.74) × 10^{18} cm^{-3} and (2.24–3.25) × 10^{18} cm^{-3}, respectively. The UV spectra were recorded at room temperature between 190 and 400 nm under static conditions by accumulating 6000 scans at an instrumental resolution of 3 nm.

The IR absorption spectra of the HFEs were recorded between 4000 and 500 cm^1 using a FTIR spectrometer (Bruker, Tensor 27) with a liquid nitrogen cooled mercury cadmium telluride detector (Blázquez et al. 2022). The instrumental resolution was set to the highest one available with the FITR spectrometer, 0.5 cm^{-1}. A single path (ℓ = 10 cm) stainless steel cell, sealed with ZnSe windows, was used to measure the absorbance at each wavenumber ($A_{\tilde{\upsilon}}$) under static conditions. The cell was filled with a pure sample of HFE-356mec3 (total pressure in the cell, P_{cell} = 1.79–12.95 mbar (≡1.34–9.70 Torr)) or HFE-236ea1, (P_{cell} = 0.96–6.64 mbar ≡ 0.72–4.98 Torr). The HFE concentration ranges were [HFE-356mec3] = (0.43–3.15) × 10^{17} cm^{-3} and [HFE-236ea1] = (0.23–1.61) × 10^{16} cm^{-3}.

A total of 3–9 spectra were used to obtain σ_{λ} and $\sigma_{\tilde{\upsilon}}$ from the slope of the Beer-Lambert's plots as shown in the examples presented in Figure S3. In addition, the integrated IR absorption cross section of a band, S_{int} (in base *e*), defined by Eq. E3, was determined from the Beer-Lambert's law (Eq. ES2) expressed in terms of the integrated absorbance, A_{int} (Eq. ES3), for comparison purposes.

$$S_{int} = \int_{band} \sigma_{\tilde{\upsilon}} d\tilde{\upsilon} \quad \text{(E3)}$$

Plots of the Beer-Lambert's law for S_{int} are presented in Figure S4 of SI.

Chemicals

Helium (99.999%, Nippon Gases), synthetic air (99.999%, Air Liquide), HFE-236ea1 (95%, Apollo Scientific and 95%, Chemspace), and CH_4 (99.995%, Sigma-Aldrich) were gases used as supplied. Aqueous solution of H_2O_2 (> 50% v/v, Scharlab) was pre-concentrated as described in (Albaladejo et al. 2002). Liquid HFE-356mec3 (> 98%, Chemspace), CH_2Cl_2 (99.8%, Sigma-Aldrich), $CH_2ClCHCl_2$ (> 98%, Cymit), and CH_3CCl_3 (95.10%, Cymit) were used after degasification by several freeze–pump–thaw cycles.

Results and discussion

Kinetic study of the OH- and Cl-reactions with HFEs

Temperature dependence of $k_{OH}(T)$

The individual $k_{OH}(T)$ for HFE-356mec3 and HFE-236ea1 are listed as a function of temperature and total pressure in Tables S1 and S2 of the SI. The rate coefficients at a single temperature provided in Table 1 are the average of the rate coefficients obtained from the slope of the plot of k'-k'_0 *vs* [HFE]. As it can be seen in Table 1, over the temperature range investigated $k_{OH}(T)$ are on the order of 10^{-14} cm^3s^{-1} for HFE-356mec3 and 10^{-15}-10^{-14} cm^3s^{-1}.

The rate coefficient $k_{OH}(T)$ increases when temperature increases. For HFE-356mec3, k_{OH}(353 K) is around three times higher than k_{OH}(263 K), while for HFE-236ea1 k_{OH}(353 K) is four times higher than k_{OH}(263 K). In Fig. 1, k'-k'_0 *vs* [HFE] plots are shown for both HFEs at 263 K and 353 K together with those at 298 K at 66.66 and 133.32 mbar.

When the kinetic data were fitted to an Arrhenius expression, the uncertainty ($\pm 2\sigma$, only statistical) in A and E_a/R parameters was very large due to the scattering of the data, as shown by Eqns. E4 and E5.

$$\mathrm{HFE-356mec3}: k_{OH}(T) = (9.93 \pm 6.65) \times 10^{-13} \exp\{-(971 \pm 213)/T\} \ cm^3s^{-1} \quad (E4)$$

$$\mathrm{HFE-236ea1}: k_{OH}(T) = (4.75 \pm 4.41) \times 10^{-13} \exp\{-(1262 \pm 602)/T\} \ cm^3s^{-1} \quad (E5)$$

By fixing the A factor, the uncertainty in E_a/R ($\pm 2\sigma$, only statistical) is reduced and the Arrhenius expressions that describe the observed T-dependence of $k_{OH}(T)$ (solid red line in Fig. 2) between 263 and 353 K are given by:

$$\mathrm{HFE-356mec3}: k_{OH}(T) = 9.93 \times 10^{-13} \exp\{-(988 \pm 35)/T\} \ cm^3s^{-1} \quad (E6)$$

$$\mathrm{HFE-236ea1}: k_{OH}(T) = 4.75 \times 10^{-13} \exp\{-(1285 \pm 22)/T\} \ cm^3s^{-1} \quad (E7)$$

The dashed blue lines in Fig. 2 represent the confidence bands at a 95% level. The observed temperature dependence of $k_{OH}(T)$ is positive in both cases, yielding ($E_a \pm 2\sigma$) of (8.2 ± 0.3) and (10.7 ± 0.2) kJ/mol^{-1} for reactions (R1) and (R2), respectively. Blázquez et al. (2022) reported an expression that relates E_a with $log(k_{OH}(298\ K))$ for a series of OH + HFE reactions. For HFE-356mec3 and HFE-236ea1, the estimated E_a using that expression are 10.3 kJ/mol^{-1} and 13.3 kJ/mol^{-1}, respectively, which are in both cases 20% higher than the experimental value determined in this work.

Table 1 Summary of the average rate coefficients obtained in this work for reactions (R1) and (R2) as a function of temperature at 133.32 mbar of He

	$k_{OH}(T)$ [a] / 10^{-14} cm^3 s^{-1}	
T/K	$CF_3CHFCF_2OCH_3$ (HFE-356mec3)	$CHF_2CHFOCF_3$ (HFE-236ea1)
263	2.25 ± 0.17	0.35 ± 0.02
273	2.71 ± 0.56	0.40 ± 0.02
283	3.14 ± 0.43	0.55 ± 0.15
298	3.68 ± 0.95 [b]	0.66 ± 0.13 [b]
313	4.75 ± 1.26	0.99 ± 0.09
333	5.76 ± 0.93	1.04 ± 0.16
353	6.19 ± 0.75	1.36 ± 0.18

[a] Uncertainties are ± 2σ statistical. [b] Including additional measurements at 66.66 mbar

Comparison of k_{OH}(298 K) for HFE-356mec3 and HFE-236ea1 with previous studies Table 2 summarizes k_{OH}(298 K) for reactions (R1) and (R2) and those previously reported in the literature. For HFE-356mec3, Urata et al. (2003) estimated k_{OH}(298 K) (1.77×10^{-14} cm^3 s^{-1}) using the modified Heicklen equation, which is half of the one reported in this work. For reaction (R2), there is only one relative kinetic measurement of k_{OH}(298 K), which was performed by Oyaro et al. (2005) using GC–MS as a detection method for HFE-236ea1 and the reference compounds used (CH_3CCl_3, CH_3CN, and CHF_2CH_2F). The reported individual k_{OH}(298 K) obtained with each reference compound were: $(6.9 \pm 1.3) \times 10^{-15}$ cm^3 s^{-1}, $(5.3 \pm 2.7) \times 10^{-15}$ cm^3s^{-1} and $(8.3 \pm 3.6) \times 10^{-15}$ cm^3 s^{-1}, respectively. Even though the scattering in the individual k_{OH}(298 K), Oyaro et al. (2005) reported a weighted average of $(6.8 \pm 1.1) \times 10^{-15}$ cm^3s^{-1}, which agrees, within the uncertainty limits, with k_{OH}(298 K) obtained in this work by an absolute kinetic method. The large uncertainty in the individual k_{OH}(298 K) reported by Oyaro et al. (2005) is greatly influenced by uncertainties in recommended k_{ref}, although they are

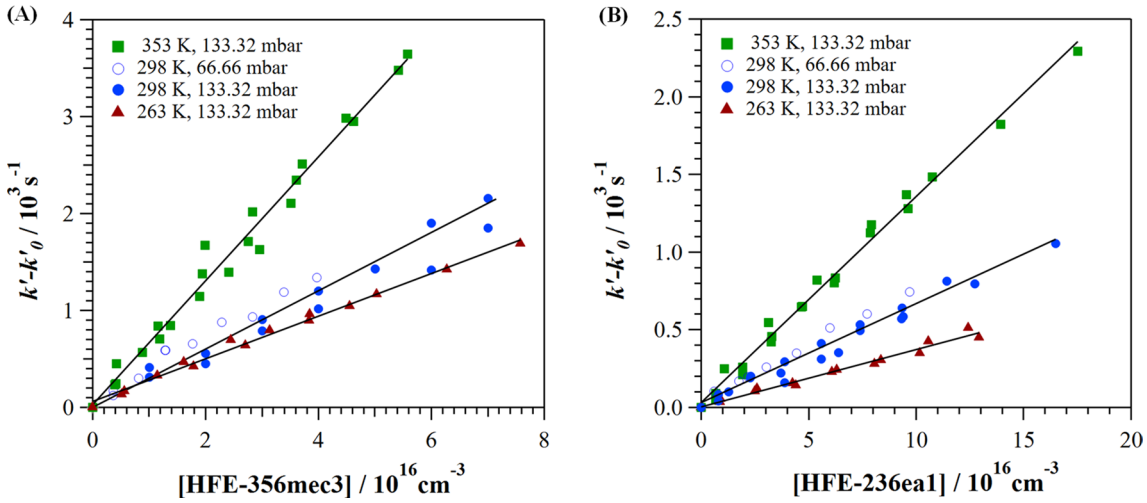

Fig. 1 Plots of equation (E1) for the OH-reaction at 263 K, 298 K, and 353 K as a function of total pressure for (**A**) HFE-356mec3 and (**B**) HFE-236ea1

well-known and currently recommended by the JPL-NASA panel (Burkholder et al. 2020).

Relative kinetics of the Cl + $CHCl_2CH_2Cl$ reaction

In Figure S5a, a relative plot according to Eq. E2 is shown for reaction (R5) for each reference compound used. The k_{Cl}(298 K)/k_{ref} ratio was obtained from the slope of such plots, as shown in Table S5. Individual k_{Cl}(298 K) obtained with both reference compounds are in good agreement, despite the large data scattering observed with CH_2Cl_2 (Figure S5b). A weighted average of $(3.08 \pm 0.36) \times 10^{-13}$ cm^3 s^{-1} is reported. The weighting factor was $1/\sigma^2$, where σ is the standard deviation in the individual k_{Cl}(298 K).

Comparison of k_{Cl}(298 K) for $CH_2ClCHCl_2$ with previous studies As shown in Table 3, k_{Cl}(298 K) reported here is in very good agreement, within the error limits, with the absolute value reported by Wine and Semmes (1983). The relative kinetic studies of Cillien et al. (1967) and Tschuikow-Roux et al. (1986) yield a much lower k_{Cl}(298 K). Note that the complex relative method used by these authors determines independently the rate coefficient for each H-abstraction channel and the values listed in Table 3 are the overall rate coefficient. Tschuikow-Roux et al. (1986) recalculated k_{Cl}(298 K) for reaction (R5) reported by Cillien et al. (1967) using the recommended value of k_{ref} for CH_4, finding an even lower value than originally reported. The reported uncertainties in k_{Cl}(298 K) for (R5) are very large

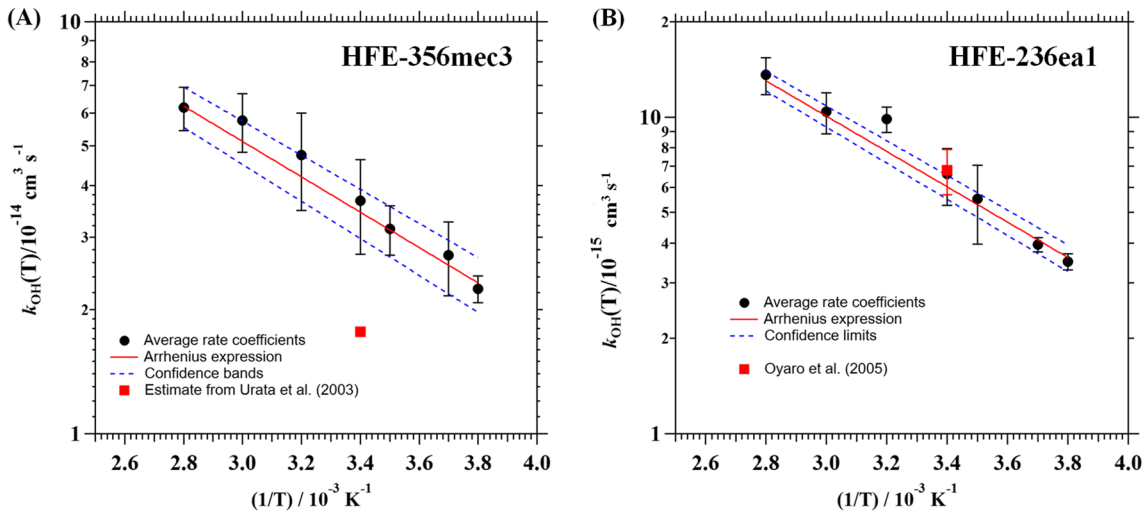

Fig. 2 Arrhenius plots of $k_{OH}(T)$ obtained in this work together with the previously reported kinetic data at room temperature for (**A**) HFE-356mec3 and (**B**) HFE-236ea1. Quoted errors are statistical ± 2σ

(see Table IV of Tschuikow-Roux et al.'s work). Note that Cillien et al. (1967) reported k_{Cl}(323 K), the lowest temperature they measured, so k_{Cl}(298 K) should be somehow lower, according to our observations. In conclusion, we have elucidated the discrepancy among previous relative studies and k_{Cl}(298 K) for $CH_2ClCHCl_2$ determined in this work was used as k_{ref} in the kinetic study of the Cl + HFE-236ea1 reaction.

Relative kinetics of Cl + HFE reactions

In Fig. 3A, the plots of Eq. E2 for the Cl-reaction with HFE-356mec3 are depicted for each reference compound. The good linearity and the zero intercept of these plots indicate the absence of interfering secondary chemistry that can affect the determination of k_{Cl}(298 K). The used k_{ref} for CH_4 and $CH_2ClCHCl_2$ were those recommended by Atkinson et al. (2006) and the obtained in this work, respectively. As shown in Fig. 3B, where both datasets are combined, there is some scattering. Nevertheless, the individual k_{Cl}(298 K) (Table S6) lies within the stated uncertainties and, thus, a weighted average is reported in Table 4. For HFE-236ea1, k_{ref} for CH_3CCl_3 was taken from the JPL-NASA evaluation panel (Burkholder et al. 2020).

Comparison of k_{Cl}(298 K) for HFE-356mec3 and HFE-236ea1 with previous studies In Table 4, k_{Cl}(298 K) obtained in this work for reactions (R3) and (R4) are compared with those reported in the literature (Oyaro et al. 2005; Papadimitriou et al. 2004). Papadimitriou et al. (2004) reported k_{Cl}(298 K) = $(2.09 \pm 1.48) \times 10^{-13}$ cm^3 s^{-1} for HFE-356mec3 at ca. 4 mbar. In this work k_{Cl}(298 K) has been determined for the first time at sea level pressure. k_{Cl}(298 K) determined by Papadimitriou et al. (2004) is in good agreement, within their large error limits, with that reported here. This means that no pressure dependence of k_{Cl}(298 K) is observed in that wide pressure range. Oyaro et al. (2005) used CH_3CCl_3 and CHF_2CH_2F as reference compounds to study the kinetics of the Cl + HFE-236ea1 reaction. These authors reported individual k_{Cl}(298 K) with three times the standard deviation ($\pm 3\sigma$) uncertainties. Despite that, these authors reported a weighted average of k_{Cl}(298 K). Even considering $\pm 2\sigma$, as in our work, the individual k_{Cl}(298 K) still present large uncertainties: $(1.1 \pm 1.4) \times 10^{-15}$ and $(2.0 \pm 4.6) \times 10^{-15}$ cm^3 s^{-1}. Current recommendations of k_{ref} for the Cl-reactions of CH_3CCl_3 and CHF_2CH_2F (Burkholder et al. 2020) present lower uncertainty factors, f(298 K) (see Table 4). Hence, considering these values in k_{ref} and f(298 K), we recalculated the weighted average k_{Cl}(298 K) from Oyaro et al.'s results to be $(1.34 \pm 0.14) \times 10^{-15}$ $cm^3 s^{-1}$ (see Table 4). This manifests the importance of reporting accurate absolute rate coefficients to reduce the uncertainty in the recommended k_{ref} which will be further used in relative measurements of k_{Cl}(298 K).

Table 2 Comparison of k_{OH}(298 K) (in 10^{-14} cm^3 s^{-1}) obtained in this work with those from the literature

HFE	k_{OH}(298 K)	Technique [c]	Reference compound	Reference
$CF_3CHFCF_2OCH_3$ (HFE-356mec3)	3.68 ± 0.95 [a]	PLP-LIF	-	This work
	1.77	Estimate	-	Urata et al. (2003)
$CHF_2CHFOCF_3$ (HFE-236ea1)	0.66 ± 0.13 [a]	PLP-LIF		This work
	0.68 ± 0.11 [b]	RR-GC/MS	CH_3CCl_3 CHF_2CH_2F	Oyaro et al. (2005)

[a] Uncertainties are $\pm 2\sigma$ statistical [b] Weighted average with $\pm 3\sigma$ statistical uncertainties. [c] PLP-LIF: pulsed laser photolysis-laser induced fluorescence; RR: relative rate method; GC/MS: gas chromatography-mass spectrometry

Table 3 Comparison of k_{Cl}(298 K) (in 10^{-13} $cm^3 s^{-1}$) reported here for $CHCl_2CH_2Cl$ with literature values

P/ mbar (Torr)	k_{Cl}(298 K)	Technique [c]	Reference compound	Reference
1013 (760)	3.21 ± 0.89 [a]	RR-FTIR	CH_4	This work
	2.96 ± 0.83 [a]	RR-FTIR	CH_2Cl_2	This work
	3.08 ± 0.36	Weighted average	-	This work
28 (16)	0.89 ± 0.54 [b]	RR-GC/FID	CH_4	Tschuikow-Roux et al. (1986)
107–335 (80–250)	1.92 [b]	RR-GC/Katharometer	$CHCl_3$	Cillien et al. (1967)
133 (100)	3.49 ± 1.44	LFP-RF	-	Wine and Semmes (1983)

[a] Uncertainties are $\pm 2\sigma$ statistical that includes the error propagation in k_{ref}. [b] See text; [c] RR, relative rate; FTIR, Fourier transform infrared; GC/FID, gas chromatography/flame ionization detection; LFP-FR, Laser flash photolysis- resonance fluorescence

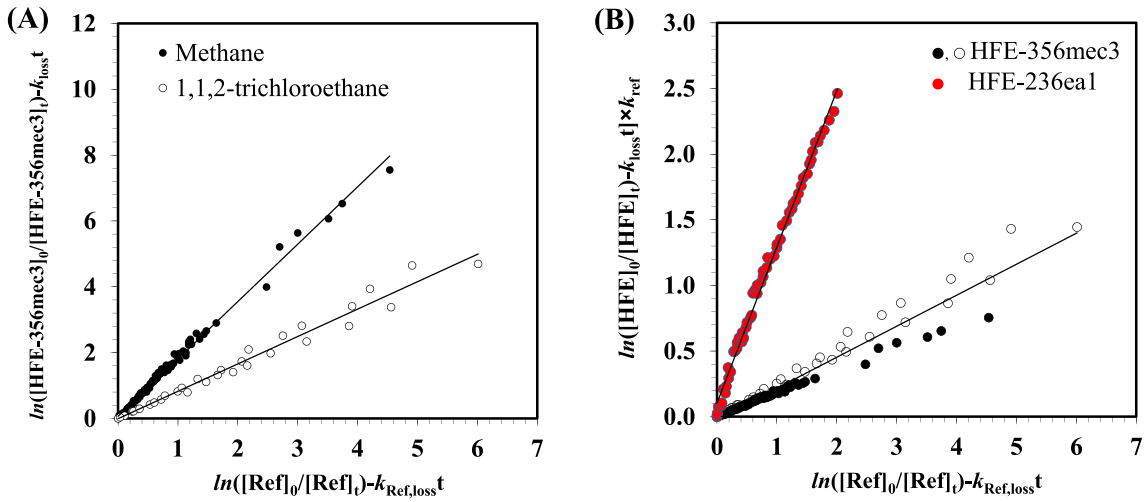

Fig. 3 Relative plots obtained for the Cl-reaction with HFE-356mec3 (**A**) and HFE-236ea1 (**B**). k_{ref} for CH_4 and $CH_2ClCHCl_2$ are listed in Table S6

Table 4 Comparison of k_{Cl}(298 K) for HFE-236ea1 and HFE-356mec3 with literature relative values

P/ mbar (Torr)	k_{Cl}(298 K) / 10^{-13} cm^3 s^{-1}	Reference compound	Reference
$CF_3CHFCF_2OCH_3$ (HFE-356mec3)			
1013 (760)	1.74 ± 0.48 [a]	CH_4	This work
1013 (760)	2.56 ± 0.33 [a]	$CHCl_2CH_2Cl$	This work
	2.30 ± 1.08 [a]	Weighted average	This work
< 4 (3)	2.09 ± 1.48 [a]	-	Papadimitriou et al. (2004)
$CHF_2CHFOCF_3$ (HFE-236ea1)			
1013 (760)	0.0119 ± 0.0001	CH_3CCl_3	This work
1013 (760)	0.011 ± 0.021 [b]	CH_3CCl_3	Oyaro et al. (2005)
	0.014 ± 0.003 [c]	recalculated	This work
1013 (760)	0.020 ± 0.070 [b]	CHF_2CH_2F	Oyaro et al. (2005)
	0.013 ± 0.014 [c]	recalculated	This work
1013 (760)	0.012 ± 0.020 [b]	Weighted average	Oyaro et al. (2005)
	0.0134 ± 0.0014[c]	Average recalculated	This work

[a] Uncertainties are ± 2σ statistical; [b] Stated uncertainties are ± 3σ. $k_{ref} = 7 \times 10^{-15}$ cm^3 s^{-1} (uncertainty given by JPL-NASA evaluation number 14 f(298 K) = 2) for CH_3CCl_3 and $k_{ref} = 4.9 \times 10^{-14}$ cm^3 s^{-1} (f(298 K) = 3) for CHF_2CH_2F; [c] Using current recommendations: $k_{ref} = 9.0 \times 10^{-15}$ cm^3 s^{-1} (uncertainty given by JPL-NASA evaluation number 19, f(298 K) = 1.15) for CH_3CCl_3 and $k_{ref} = 2.5 \times 10^{-14}$ cm^3 s^{-1} (f(298 K) = 1.3) for CHF_2CH_2F (Burkholder et al. 2020)

Comparison of the OH- and Cl-reactivity of HFEs with their structurally analogous HFCs

The equivalent HFC to $CF_3CHFCF_2OCH_3$ (HFE-356mec3) is $CF_3CHFCF_2CH_3$ (HFC-356mec) but no information is available, as far as we know. When comparing k_{OH}(298 K) and k_{Cl}(298 K) determined in this work for HFE-356mec3 with those reported by Barry et al. (1997) for the analogue HFC, HFC-365mfc (Table S7), it is clear that the presence of the ether group increases both rate coefficients. Particularly for the Cl-reaction, k_{Cl}(298 K) increases more than two orders of magnitude with respect to the HFC. Concerning the temperature dependence of k_{OH}(T), E_a for the OH-reactions of HFE-356mec3 and its HFC analogue are similar, within the experimental uncertainties. For $CHF_2CHFOCF_3$ (HFE-236ea1), the equivalent HFC is CHF_2CHFCF_3 (HFC-236ea). The decrease in k_{OH}(298 K) for HFC-236ea reported by Atkinson et al. (2006) is less pronounced than that for HFE-356mec3. However, the same trend is observed in E_a. No kinetic data has been found in the literature for the Cl + HFC-236ea reaction.

Absorption cross sections in the UV and IR region

HFEs weakly absorb at wavelengths longer than 200 nm (Figures S6 and S7), especially HFE-236ea1 which presents σ_λ lower than 1×10^{-23} cm^2 molecule^{-1} at $\lambda>210$ nm. In contrast, HFE-356mec3 presents higher absorption at $\lambda>210$ nm, $\sigma_{210nm}=(1.08\pm0.04)\times10^{-21}$ cm^2. σ_λ are listed at 0.5 nm intervals in the Excel spreadsheet provided in the SI. Considering σ_λ at the photolysis wavelength ($\sigma_{248nm}=(1.17\pm0.35)\times10^{-22}$ cm^2), the laser fluences and [HFE] employed in this work, HFE-356mec3 and HFE-236ea1 are not photolyzed during the kinetic experiments. A photolysis quantum yield for HFEs of 1 was assumed.

In the mid-IR region, the obtained $\sigma_{\tilde{\nu}}$ for HFE-356mec3 and HFE-236ea1 are listed in the Excel spreadsheet provided in the SI between 500 and 4000 cm^{-1} and depicted in Figure S8. In the 2700–1600 cm^{-1} range, both HFEs present negligible absorption, and a very weak band in the 3100–2700 cm^{-1} range. The obtained IR spectra between 500 and 1500 cm^{-1} in terms of $\sigma_{\tilde{\nu}}$ for both HFEs are depicted as black lines in Figure S9, while IR spectra reported in the literature are plotted as blue lines.

In Table S8, the value and the position of the absorption peak ($\sigma_{\tilde{\nu},max}$) are listed together with those reported in the literature. $\sigma_{\tilde{\nu},max}$ for HFE-356mec3 and HFE-236ea1 is located at 1211.9 cm^{-1} and 1136 cm^{-1}, respectively. For HFE-356mec3, the position of $\sigma_{\tilde{\nu},max}$ is in excellent agreement with the high-resolution study of Le Bris et al. (2020) at 305 K (1211.9 cm^{-1}), which reports $\sigma_{\tilde{\nu},max}$ 7% higher than ours. For HFE-236ea1, Oyaro et al. (2005) reported that $\sigma_{\tilde{\nu},max}$ was located at 1136 cm^{-1} which is in excellent agreement with $\sigma_{\tilde{\nu},max}$ determined in this work although $\sigma_{\tilde{\nu},max}$ at 1136 cm^{-1} is 21% lower than ours. With respect to $S_{int,}$ it is summarized in Table S8 to compare with previous works. For HFE-356mec3, S_{int}(1650–660 cm^{-1}) is 7% lower than that of Le Bris et al. (2020). For HFE-236ea1, S_{int}(1600–465 cm^{-1}) reported by Oyaro et al. (2005) is around 22% lower than the reported in this work, consequence of their lower IR absorption cross sections in the 1100–1300 cm^{-1} region. Additional experiments carried out at an instrumental resolution of 1 cm^{-1} provide the same IR absorption cross section for HFE-236ea1 (See Figure S10). Thus, the instrumental resolution of the FTIR spectrometer used is not the source of the observed discrepancy.

Atmospheric implications

Tropospheric lifetimes, τ_{tropos}

As shown in Figure S7, the investigated HFEs do not appreciably absorb in the solar actinic UV region ($\lambda>290$ nm), which may indicate that their degradation by UV photolysis in the troposphere can be negligible, especially if their photolysis quantum yield is very low in the actinic region. Further studies would be necessary to confirm this assertion. Therefore, the tropospheric lifetime of HFE-356mec3 and HFE-236ea1, τ_{tropos}, mainly depends on their reactivity towards the atmospheric oxidants (OH, Cl, O_3 or NO_3).

$$\frac{1}{\tau_{tropos}}=\sum_{Ox}\frac{1}{\tau_{Ox}} \quad \text{(E8)}$$

τ_{Ox} is the lifetime due to the reaction of HFE-356mec3 and HFE-236ea1 with the oxidant, Ox. To our knowledge, the rate coefficients for the reactions of O_3 and NO_3 with the HFEs are not known, although they are expected to be very low compared to the reaction with OH and Cl. Thus, here we consider only the removal by OH and Cl, and τ_{Ox} is denoted as τ_{OH} and τ_{Cl}.

Two scenarios were considered to estimate the tropospheric lifetime of HFEs due to homogeneous reactions: a global atmosphere (scenario *i*) and a coastal atmosphere at dawn (scenario *ii*), where the Cl chemistry can play a significant role. The atmospheric lifetime due to the reaction of HFEs with OH determines the degree of homogeneity in their distribution in the atmosphere. For long-lived gases (τ_{OH} greater than a few months), the atmospheric lifetime is usually estimated relative to CH_3CCl_3 at the tropospheric mean temperature, 272 K (Spivakovsky et al. 2000):

$$\tau_{OH}(\text{HFE})=\frac{k_{OH+CH_3CCl_3}(272\text{ K})}{k_{OH}(272\text{ K})}\times\tau_{OH}(CH_3CCl_3) \quad \text{(E7)}$$

where $\tau_{OH}(CH_3CCl_3)$ is the atmospheric lifetime of CH_3CCl_3 due to reaction with OH (5.99 years) and $k_{OH+CH_3CCl_3}$(272 K) is 6.03×10^{-15} cm^3 s^{-1} (Hodnebrog et al. 2020). The rate coefficient for (R1) and (R2) at 272 K, k_{OH}(272 K), were obtained from equations E5 and E6, respectively. For HFE-356mec3, k_{OH}(272 K)= 2.63×10^{-14} cm^3 s^{-1} and for HFE-236ea1, k_{OH}(272 K)= 4.22×10^{-15} cm^3 s^{-1}. The estimated τ_{OH} for HFE-356mec3 and HFE-236ea1 is 1.4 and 8.6 years, respectively.

To evaluate the relative importance of the degradation of the HFEs by Cl with respect to the OH reaction, the estimation of the atmospheric lifetime of HFEs due to Cl-reaction, τ_{Cl}(HFE), was carried out using Eq. E9, the rate coefficients obtained in this work at 298 K and the 24-h average Cl concentration (see Table S9).

$$\tau_{Cl}(\text{HFE})=\frac{1}{k_{Cl}(298\text{ K})[Cl]} \quad \text{(E9)}$$

Estimates of τ_{Cl} for HFE-356mec3 and HFE-236ea1 are 138 years and 26605 years, respectively. Although in this estimation the temperature conditions of the surface were used instead of the tropospheric mean temperature, the global removal of these HFEs is dominated by the reaction

with OH radicals. Therefore, the global atmospheric lifetime can be taken as τ_{OH} and were considered in the calculation of *GWP* (see "Other potential atmospheric sinks of HFE-236ea1 and HFE-356mec3" section).

In a coastal atmosphere at dawn, τ_{Cl}(HFE) and τ_{OH}(HFE) were estimated using Eq. E9 and E10, respectively, where [Cl] and [OH] are the concentrations of the oxidants at the first hours of the day (see Table S9).

$$\tau_{OH}(\text{HFE}) = \frac{1}{k_{\text{OH}}(298\ \text{K})[\text{OH}]} \quad \text{(E10)}$$

Even though τ_{Cl}(HFE) are reduced two orders of magnitude (see Table S9), the OH reaction is still the main degradation route for HFE-356mec3 and HFE-236ea1 at the first hours of the day.

Other potential atmospheric sinks of HFE-236ea1 and HFE-356mec3

Other potential removal processes for these HFEs in the troposphere may be the direct dissolution of the gaseous pollutant into seawater or transfer from rainwater. Fluorinated ethers are expected to be very soluble in water, according to the estimation of the water solubility from US Environmental Protection Agency's EPISuite™. For HFE-356mec3, the water solubility is estimated to be 522.2 mg/L at 25 ºC, while for HFE-236ea1 it is estimated to be 5946 mg/L. These values are in fresh water and can be taken as upper limits, since the ocean salinity may decrease the water solubility of the HFEs, as estimated for several HFCs by Li et al. (2019). Therefore, if these HFEs are uptaken onto the ocean and dissolved they could affect their atmospheric residence time (Wang et al. 2023) since it involves not only atmospheric loss rates (i.e., reaction with OH) but also ocean processes (such as ocean uptake and outgassing) and other processes (such as stratospheric photochemistry).

If these HFEs were rainout, these pollutants may be transferred into the ocean. However, calculations made to assess the contribution of wet deposition to the atmospheric removal of these HFEs show that it is negligible compared to chemical removal by OH radicals. Based on the EPISuite estimated Henry's law constants for $CF_3CHFCF_2OCH_3$ and $CHF_2CHFOCF_3$, $k_{pc} = 0.3487$ and 0.02826 atm m^3/mole, respectively, at 25 ºC, their lifetime due to wet deposition is on the order of thousands of years. This lifetime was estimated from Eqn. (E11) (Jiménez et al. 2009).

$$\tau_{wet} = \frac{z(km)}{v_{precip}(mmyr^{-1})R(atmM^{-1}K^{-1})T(K)k_{cp}(Matm^{-1})}10^6 mm/km \quad \text{(E11)}$$

where $k_{cp} = 0.0029$ M atm^{-1} for $CF_3CHFCF_2OCH_3$ and 0.035 M atm^{-1} for $CHF_2CHFOCF_3$ at 25 ºC and the annual average precipitation rate (v_{precip}) was taken for Spain over the 1991–2020 period (636 mm/yr). The individual lifetime for $CF_3CHFCF_2OCH_3$ and $CHF_2CHFOCF_3$ due to wet deposition is extremely long (11,213 yrs and 909 at 0.5 km altitude and 25ºC) to affect the atmospheric overall lifetime.

On the other hand, as the transport time from troposphere to stratosphere is of several years, these long-lived HFEs can be then transported to the stratosphere. Thus, the dynamical coupling between stratosphere and troposphere cannot be dismissed. The potential photolysis rate (*J*) of HFE-356mec3 and HFE-236ea1 in the stratosphere strongly depends on the photolysis quantum yield. Considering the UV absorption cross sections determined in this work between 190 and 400 nm and the spectral actinic flux between 180 and 400 nm at an altitude of 50 km (Demore et al. 1997), in the most favorable scenario (a photolysis quantum yield of 1) *J* would be 1.7×10^{-6} s^{-1} and 4.8×10^{-7} s^{-1}, respectively. These *J* values translate in a stratospheric lifetime for HFE-356mec3 and HFE-236ea1 due to photolysis of around 7 and 24 days. But these numbers may not be realistic if the photolysis quantum yield is much lower than unity, and have to be taken cautiously. Further photochemical studies would be needed to determine the photolysis quantum yield of these HFEs as a function of wavelength.

Radiative efficiencies and GWPs

Using the same methodology as in our previous works (Blázquez et al. 2022, 2017), *RE*s (in W m^{-2} $ppbv^{-1}$) and *GWP*s relative to CO_2 of HFEs were calculated for a time horizon of 100 years, *GWP*(*100 yrs*). In this work, the instantaneous *RE*s were corrected with τ_{OH}(HFE) as explained by Shine and Myhre (2020). The fractional correction factors were calculated from τ_{OH}(HFE) in scenario *i* of Table S9 to be 0.793 for HFE-356mec3 and 0.948 for HFE-236ea1. The obtained lifetime-corrected *RE*s are summarized in Table 5. As shown, *RE* for HFE-236ea1 is higher (34%) than that for HFE-356mec3, mainly due to the smaller correction of the instantaneous *RE* (5% versus 21%).

For HFE-356mec3, as τ_{OH}(HFE) is shorter than previously reported, the lifetime-corrected *RE* is lower than those reported (0.29–0.31 W m^{-2} $ppbv^{-1}$) (Burkholder et al. 2018; Hodnebrog et al. 2020; Le Bris et al. 2020). The overestimation of *RE* for HFE-356mec3 previously reported (7–13% higher) is due to the consideration of the atmospheric lifetime of $CF_3CHFCF_2OCH_3$ to be equal to that of $CHF_2CF_2OCH_2$ because no experimental data were available. In addition, Burkholder et al. (2018), considered the *RE* for HFE-356mec3 given by Hodnebrog et al. (2013). For HFE-236ea1, Oyaro et al. (2005) reported an instantaneous *RE* (0.35 W m^{-2} $ppbv^{-1}$) according to the procedure given by Pinnock et al. (1995) Applying the fractional correction factor to the instantaneous *RE* reported by Oyaro et al. (2005) the resulting *RE* (0.40 W m^{-2} $ppbv^{-1}$) is in

Table 5 Lifetimes due to OH reaction, lifetime-corrected *RE*s, and *GWP*s at a time horizon of 100 years for the investigated HFEs and their analogue HFCs

Species *i*	τ_{OH}/ years	RE_i / W m^{-2} $ppbv^{-1}$	GWP_i(*100 years*)	Reference
$CF_3CHFCF_2OCH_3$	1.4	0.27	143	This work
HFE-356mec3	2.5	0.30	250	Burkholder et al. (2018)
	2.6	0.29	277	Hodnebrog et al. (2020)
	2.5	0.31	260	Le Bris et al. (2020)
$CF_3CH_2CF_2CH_3$ HFC-365mfc	8.7	0.22	804	Hodnebrog et al. (2020)
$CHF_2CHFOCF_3$	8.6	0.41	1473	This work
HFE-236ea1	9.8	0.40*	1621	Oyaro et al. (2005)
CHF_2CHFCF_3 HFC-236ea	11.4	0.30	1570	Hodnebrog et al. (2020)

* Original data have been corrected here with the lifetime

excellent agreement with the value determined in this work (0.41 W m^{-2} $ppbv^{-1}$).

The *GWP*(*100 yrs*) values in Table 5 were obtained using the lifetime-corrected *RE*s and τ_{OH}(HFE) from scenario *i* of Table S9. As shown, *GWP*(*100 yrs*) for HFE-236ea1 is much higher than that for HFE-356mec3, because both *RE* and τ_{OH}(HFE) are higher. *GWP*(*100 yrs*) for HFE-356mce3 calculated in this work is 143, around 45% lower than the values from the literature (Burkholder et al. 2018; Hodnebrog et al. 2020; Le Bris et al. 2020). This is a consequence of the combined effect of a higher τ_{OH}(HFE) and *RE*. For HFE-236ea1, *GWP(100 yrs)* from corrected results from Oyaro et al. (2005) is still 9% higher than that from this work. When compared *GWP*(*100 yrs*) of HFE-236ea1 with that of its structurally analogue HFC, CHF_2CHFCF_3 (HFC-236ea), it is reduced 6%. However, using the results from Oyaro et al. (2005) would *GWP*(*100 yrs*) of HFE-236ea1 would increase 3% with respect to HFC-236ea. This indicates that accurate lifetimes and *RE*s are necessary to establish the impact of a pollutant on global warming. Similarly, the impact on the global warming of the structurally analogue HFC for HFE-356mec3, $CF_3CHFCF_2CH_3$ (HFC-356mec) has to be evaluated, since no information is available, as far as we know. Nevertheless, as shown in Table 5, *GWP*(*100 yrs*) for an HFC with the same number of C-F bonds as HFC-356mec, i. e. $CF_3CH_2CF_2CH_3$ (HFC-365mfc), is ca. 6 times higher than that for HFE-356mec3.

Conclusions

This work reports the first determination of the rate coefficient $k_{OH}(T)$ for the OH-reaction with $CF_3CHFCF_2OCH_3$ (HFE-356mec3) and $CHF_2CHFOCF_3$ (HFE-236ea1) as a function of temperature (263–353 K). A positive temperature dependence of $k_{OH}(T)$ was observed with activation energies of (8.2 ± 0.3) and (10.7 ± 0.2) kJ/mol^{-1} for HFE-356mec3 and HFE-236ea1, respectively. At room temperature, k_{OH}(298 K) is $(3.68 \pm 0.95) \times 10^{-14}$ cm^3s^{-1} for HFE-356mec3 and $(6.6 \pm 1.3) \times 10^{-15}$ cm^3s^{-1} for HFE-236ea1. No pressure dependence of $k_{OH}(T)$ was observed in the 66.66–133.32 mbar range. In addition, the rate coefficient for the corresponding Cl-reactions at 298 K and 1013 mbar (760 Torr), k_{Cl}(298 K), was determined to be $(2.30 \pm 1.08) \times 10^{-13}$ cm^3s^{-1} for HFE-356mec3 and $(1.19 \pm 0.10) \times 10^{-15}$ cm^3s^{-1} for HFE-236ea1. At 298 K, HFE-356mec3 reacts 6 times faster with Cl atoms than with OH radicals. However, HFE-236ea1 reacts more than 5 times faster with OH than with Cl.

Concerning the UV photolysis in the troposphere of the investigated HFEs, as they do not appreciably absorb at wavelengths longer than 200 nm ($\sigma_\lambda < 1 \times 10^{-21}$ cm^2 for HFE-356mec3 and $< 2.5 \times 10^{-22}$ cm^2 for HFE-236ea1), it is expected that this removal process is not important. However, the photolysis rate of these HFEs would depend on the photolysis quantum yield which is not known. The tropospheric lifetimes for HFE-356mec3 and HFE-236ea1, estimated relative to CH_3CCl_3, were 1.4 and 8.6 years, respectively, being the main removal pathway for these HFEs the reaction with OH radicals. From the IR absorption cross sections determined in this work between 4000 and 500 cm^{-1} for HFE-356mec3 and HFE-236ea1, their lifetime-corrected radiative efficiency was calculated to be 0.27 and 0.41 W m^{-2} $ppbv^{-1}$, respectively. At a time horizon of 100 years, HFE-356mec3 and HFE-236ea1 present GWPs relative to CO_2 of 143 and 1473, respectively, which implies that for the same amount of CO_2 and HFE emitted (1 kg) to the atmosphere, the contribution to global warming of these HFEs would be more than 100 times higher than CO_2 effect for HFE-356mec3 and more than 1000 times higher for HFE-236ea1. Therefore, HFE-356mec3 and HFE-236ea1 would largely impact on the radiative forcing of the atmosphere, if they become widespread increasing their atmospheric concentration.

Supplementary Information The online version contains supplementary material available at https://doi.org/10.1007/s11356-024-34374-8.

Acknowledgements The authors would like to thank Prof. Claus J. Nielsen and Dr. Karine Le Bris for providing their IR absorption cross sections of HFE-356mec3 and HFE-236ea1. The authors also thank Prof. Juan Tejeda from UCLM for performing the purity analysis by NMR of HFE-356mec3. M. Asensio also acknowledges the regional government of Castilla-La Mancha through the CINEMOL project (Ref.: SBPLY/19/180501/000052) co-funded by the European Regional Development Fund (FEDER) and the University of Castilla-La Mancha (Ref.: 2022-GRIN-34143) for funding her contracts during the performance of these experiments.

Author contributions Sara Espinosa and María Asensio carried out the experiments, made the analysis and interpretation of data and prepared the original draft. María Antiñolo contributed to the conceptualization and supervision of the experiments, and the preparation and review of the original draft. José Albaladejo reviewed and edited the original draft. Elena Jiménez contributed to the conceptualization and supervision of the experiments, reviewed and edited the original draft, and acquired the funds and managed the funded projects.

Funding This work has been supported by the regional government of Castilla-La Mancha through the CINEMOL project (Ref.: SBPLY/19/180501/000052) and INTERESFERA project (Ref.: SBPLY/23/180225/000054), both co-funded by the European Regional Development Fund (FEDER). We also acknowledge the University of Castilla-La Mancha for funding this work through the *Ayudas para la financiación de actividades de investigación dirigidas a grupos* (Ref.: 2022-GRIN-34143) co-funded by FEDER funds.

Data availability The manuscript has data included as electronic supplementary material.

Declarations

Ethical approval and consent to participate Not applicable.

Consent for publication Not applicable.

Competing interests The authors have no competing interests to declare that are relevant to the content of this article.

References

Albaladejo J, Ballesteros B, Jiménez E, Martín P, Martínez E (2002) A PLP–LIF kinetic study of the atmospheric reactivity of a series of C4–C7 saturated and unsaturated aliphatic aldehydes with OH. Atmos Environ 36:3231–3239. https://doi.org/10.1016/S1352-2310(02)00323-0

Antiñolo M, González S, Ballesteros B, Albaladejo J, Jiménez E (2012) Laboratory Studies of $CHF_2CF_2CH_2OH$ and $CF_3CF_2CH_2OH$: UV and IR Absorption Cross Sections and OH Rate Coefficients between 263 and 358 K. J Phys Chem A 116:6041–6050. https://doi.org/10.1021/jp2111633

Antiñolo M, Asensio M, Albaladejo J, Jiménez E (2020) Gas-phase reaction of trans-2-Methyl-2-butenal with Cl: Kinetics, gaseous products, and SOA formation. Atmosphere 11. https://doi.org/10.3390/atmos11070715

Asensio M, Antiñolo M, Blázquez S, Albaladejo J, Jiménez E (2022) Evaluation of the daytime tropospheric loss of 2-methylbutanal. Atmos Chem Phys 22:2689–2701. https://doi.org/10.5194/acp-22-2689-2022

Asensio M, Blázquez S, Antiñolo M, Albaladejo J, Jiménez E (2023) Atmospheric impact of 2-methylpentanal emissions : Kinetics, photochemistry, and formation of secondary pollutants. Atmos Chem Phys 23:14115–14126. https://doi.org/10.5194/acp-23-14115-2023

Atkinson R, Baulch DL, Cox RA, Crowley JN, Hampson RF, Hynes RG, Jenkin ME, Rossi MJ, Troe J (2006) Evaluated kinetic and photochemical data for atmospheric chemistry: Volume II – gas phase reactions of organic species. Atmos Chem Phys 6:3625–4055. https://doi.org/10.5194/acp-6-3625-2006

Ballesteros B, Jiménez E, Moreno A, Soto A, Antiñolo M, Albaladejo J (2017) Atmospheric fate of hydrofluoroolefins, $C_xF_{2x+1}CH{=}CH_2$ (x = 1,2,3,4 and 6): Kinetics with Cl atoms and products. Chemosphere 167:330–343. https://doi.org/10.1016/j.chemosphere.2016.09.156

Barry J, Locke G, Scollard D, Sidebottom H, Treacy J, Clerbaux C, Colin R, Franklin J (1997) 1,1,1,3,3,-pentafluorobutane (HFC-365mfc): Atmospheric degradation and contribution to radiative forcing. Int J Chem Kinet 29:607–617. https://doi.org/10.1002/(SICI)1097-4601(1997)29:8

Blázquez S, Antiñolo M, Nielsen OJ, Albaladejo J, Jiménez E (2017) Reaction kinetics of $(CF_3)_2CFCN$ with OH radicals as a function of temperature (278–358 K): A good replacement for greenhouse SF_6? Chem Phys Lett 687:297–302. https://doi.org/10.1016/j.cplett.2017.09.039

Blázquez S, González D, Neeman EM, Ballesteros B, Agúndez M, Canosa A, Albaladejo J, Cernicharo J, Jiménez E (2020) Gas-phase kinetics of CH_3CHO with OH radicals between 11.7 and 177.5 K. Phys Chem Chem Phys 22:20562–20572. https://doi.org/10.1039/d0cp03203d

Blázquez S, Espinosa S, Antiñolo M, Albaladejo J, Jiménez E (2022) Kinetics of $CF_3CH_2OCH_3$ (HFE-263fb2), $CHF_2CF_2CH_2OCH_3$ (HFE-374pcf), and $CF_3CF_2CH_2OCH_2$ (HFE-365mcf3) with OH radicals, IR absorption cros. Phys Chem Chem Phys 24:14354–14364. https://doi.org/10.1039/d2cp00160h

Burkholder JB (Lead Author), Hodnebrog Ø, Orkin VL (2018) Summary of abundances, lifetimes, Ozone Depletion Potentials (ODPs), Radiative Efficiencies (REs), Global Warming Potentials (GWPs), and Global Temperature Change Potentials (GTPs), Appendix A in Scientific assessment of ozone depletion: 2018. Global ozone research and monitoring project-report no. 58. world meteorological organization, Geneva, Switzerland

Burkholder JB, Sander SP, Abbatt JPD, Barker JR, Huie RE, Kolb CE, Kurylo MJ, Orkin VL, Wilmouth DM, Wine PH (2020) Chemical Kinetics and Photochemical Data for Use in Atmospheric Studies, Evaluation No. 19. JPL Publ 19–5:1–153

Ceacero-Vega AA, Ballesteros B, Bejan I, Barnes I, Jiménez E, Albaladejo J (2012) Kinetics and mechanisms of the tropospheric reactions of menthol, borneol, fenchol, camphor, and fenchone with hydroxyl radicals (OH) and chlorine atoms (Cl). J Phys Chem A 116:4097–4107. https://doi.org/10.1021/jp212076g

Cillien C, Goldfinger P, Huybrechts G, Martens G (1967) Hydrogen abstraction from chlorinated ethanes by chlorine atoms. Int J Chem Kinet 5:539–543. https://doi.org/10.1002/kin.550050404

Demore WB, Howard CJ, Sander SP, Ravishankara AR, Golden DM, Kolb CE, Hampson RF, Molina MJ, Kurylo MJ (1997) Chemical kinetics and photochemical data for use in stratospheric modeling. Evaluation No. 12 JPL Publ 97-4:1–269

Hodnebrog, Etminan M, Fuglestvedt JS, Marston G, Myhre G, Nielsen CJ, Shine KP, Wallington TJ (2013) Global warming potentials and radiative efficiencies of halocarbons and related compounds: A comprehensive review. Rev Geophys 51:300–378. https://doi.org/10.1002/rog.20013

Hodnebrog, Aamaas B, Fuglestvedt JS, Marston G, Myhre G, Nielsen CJ, Sandstad M, Shine KP, Wallington TJ (2020) Updated Global Warming Potentials and Radiative Efficiencies of Halocarbons and Other Weak Atmospheric Absorbers. Rev Geophys. https://doi.org/10.1029/2019RG000691

Jiménez E, Lanza B, Antiñolo M, Albaladejo J (2009) Photooxidation of leaf-wound oxygenated compounds, 1-penten-3-ol, (z)-3-hexen-1-ol, and 1-penten-3-one, initiated by OH radicals and sunlight. Environ Sci Technol 43:1831–1837. https://doi.org/10.1021/es8027814

Le Bris K, DeZeeuw J, Godin PJ, Strong K (2020) Radiative efficiency and global warming potential of the hydrofluoroether HFE-356mec3 ($CH_3OCF_2CHFCF_3$) from experimental and theoretical infrared absorption cross-sections. J Mol Spectrosc 367:111241. https://doi.org/10.1016/j.jms.2019.111241

Li P, Mühle J, Montzka SA, Oram DE, Miller BR, Weiss RF, Fraser PJ, Tanhua T (2019) Atmospheric histories, growth rates and solubilities in seawater and other natural waters of the potential transient tracers HCFC-22, HCFC-141b, HCFC-142b, HFC-134a, HFC-125, HFC-23, PFC-14 and PFC-116. Ocean Sci 15:33–60. https://doi.org/10.5194/os-15-33-2019

Orkin VL, Villenave E, Huie RE, Kurylo MJ (1999) Atmospheric lifetimes and global warming potentials of hydrofluoroethers: Reactivity toward OH, UV spectra, and IR absorption cross sections. J Phys Chem A 103:9770–9779. https://doi.org/10.1021/jp991741t

Oyaro N, Sellevåg SR, Nielsen CJ (2005) Atmospheric chemistry of hydrofluoroethers: Reaction of a series of hydrofluoroethers with OH radicals and Cl atoms, atmospheric lifetimes, and global warming potentials. J Phys Chem A 109:337–346. https://doi.org/10.1021/jp047860c

Papadimitriou VC, Kambanis KG, Lazarou YG, Papagiannakopoulos P (2004) Kinetic Study for the Reactions of Several Hydrofluoroethers with Chlorine Atoms. J Phys Chem A 108:2666–2674. https://doi.org/10.1021/jp031081z

Pinnock S, Hurley MD, Shine KP, Wallington TJ, Smyth TJ (1995) Radiative forcing of climate by hydrochlorofluorocarbons and hydrofluorocarbons. J Geophys Res 100:227–238. https://doi.org/10.1029/95jd02323

Shine KP, Myhre G (2020) The Spectral Nature of Stratospheric Temperature Adjustment and its Application to Halocarbon Radiative Forcing. J Adv Model Earth Syst 12:1–16. https://doi.org/10.1029/2019MS001951

Spivakovsky CM, Logan JA, Montzka SA, Balkanski YJ, Foreman-Fowler M, Jones DBA, Horowitz LW, Fusco AC, Brenninkmeijer CAM, Prather MJ, Wofsy SC, McElroy MB (2000) Three-dimensional climatological distribution of tropospheric OH: Update and evaluation. J Geophys Res Atmos 105:8931–8980. https://doi.org/10.1029/1999JD901006

Tsai W (2005) Environmental risk assessment of hydrofluoroethers (HFEs). J Hazard Mater 119:69–78. https://doi.org/10.1016/j.jhazmat.2004.12.018

Tschuikow-Roux E, Faraji F, Niedzielski J (1986) Rate constants and kinetic isotope effects for hydrogen/deuterium abstraction by chlorine atoms from the chloromethyl group in CH_2ClCH_2Cl, CD_2ClCD_2Cl, $CH_2ClCHCl_2$, and $CH_2ClCDCl$<s. Int J Chem Kinet 18:513–527. https://doi.org/10.1002/kin.550180502

Urata S, Takada A, Uchimaru T, Chandra AK (2003) Rate constants estimation for the reaction of hydrofluorocarbons and hydrofluoroethers with OH radicals. Chem Phys Lett 368:215–223. https://doi.org/10.1016/S0009-2614(02)01718-9

Wang P, Solomon S, Lickley M, Scott JR, Weiss RF, Prinn RG (2023) On the Influence of Hydroxyl Radical Changes and Ocean Sinks on Estimated HCFC and HFC Emissions and Banks. Geophys Res Lett 50. https://doi.org/10.1029/2023GL105472

Wine PH, Semmes DH (1983) Kinetics of Cl(2PJ) Reactions with Chloroethanes CH_3CH_2Cl, CH_3CHCl_2, CH_2ClCH_2Cl, and $CH_2ClCHCl_2$. J Phys Chem 87:3572–3578

Authors and Affiliations

Sara Espinosa[1,2] · María Asensio[1,2] · María Antiñolo[1,2] · José Albaladejo[1,2] · Elena Jiménez[1,2]

✉ Elena Jiménez
Elena.Jimenez@uclm.es

[1] Facultad de Ciencias y Tecnologías Químicas, Departamento de Química Física, Universidad de Castilla-La Mancha (UCLM), Avda. Camilo José Cela, 1B, 13071 Ciudad Real, Spain

[2] Instituto de Investigación en Combustión y Contaminación Atmosférica (ICCA), Universidad de Castilla-La Mancha (UCLM), Camino de Moledores, S/N, 13071 Ciudad Real, Spain